POLARIMETRIC STUDY OF THE IC 2944 STELLAR AGGREGATE[1]

E. I. VEGA[2]
Instituto de Astronomía y Física del Espacio, CONICET, Argentina, and Programa de Fotometría y Estructura Galáctica, CONICET
Electronic mail: irene@iafe.uba.ar

A. M. ORSATTI[2]
Facultad de Ciencias Astronómicas y Geofísicas, Universidad Nacional de La Plata, 1900 La Plata, Argentina, and Programa de Fotometría y Estructura Galáctica, CONICET
Electronic mail: aorsatti@fcaglp.edu.ar

H. G. MARRACO[2]
Comisión Nacional de Actividades Espaciales, and CONICET, Argentina
Electronic mail: hmarraco@conae.gov.ar

Received 1994 April 21; revised 1994 July 5

ABSTRACT

We present *UBVRI* polarimetric observations of 30 stars belonging to the rich stellar aggregate IC 2944, which is embedded in an extensive H II region. Within the galaxy, it is located at the inner border of the Carina spiral feature. To analyze the characteristics of the interstellar material associated with the aggregate, we have separated the *frontside* contribution of both color excesses and polarizations, leaving the *intra-arm* values of these quantities. We have found that the foreground polarization in the direction to IC 2944 is normal and has a $\overline{\lambda_{max}}$ value of $0.550 \pm 0.025 \mu$. Its average direction in equatorial coordinates is 91°.2. About half of the stars not considered to be *frontside* have some indication of intrinsic polarization. Interpreting the polarization of the rest as *intra-arm* polarization, we find that Ardeberg & Maurice's Groups I, II, and III cannot be separated in terms of polarization data and that the Bright Rim Group and Group IV are significantly different from the others. Finally, stars in Groups I, II, III, and IV show that the *intra-arm* (beyond 1.4 kpc) magnetic field is essentially contained in the plane of the sky.

1. INTRODUCTION

IC 2944 is a rich stellar aggregate centered on HD 101205 ($l = 294°.8$, $b = -1°.7$), which is embedded in an extensive H II region (RWC 62). Within the galaxy, it is located at the inner border of the Carina spiral feature.

There exists some dispute about the physical entity of the aggregate. Ardeberg & Maurice (1977a, b, 1980) find that the majority of the stars belong to various stellar groups distributed along the line of sight, while Perry & Landolt (1986) show evidence which indicates that the aggregate is an apparent stellar concentration due to the superposition of early-type field stars falling on our line of sight to the aggregate. Finally, Walborn (1987) finds that at least the O stars in the field of IC 2944 constitute a significant physical cluster, the energy source of the H II region.

The aim of this investigation is to study the distribution and characteristics of the interstellar dust associated with the aggregate. To do that, we present multicolor polarimetric measures for 30 stars belonging to IC 2944, to determine the amount and direction of the linear polarization towards the aggregate. By observing the amount of the interstellar polarization in the *UBVRI* bandpasses, the wavelength of maximum polarization is computed and then analyzed in relation to the optical properties and characteristic particle-size distribution of the grains responsible for the polarization.

2. THE OBSERVATIONS

The stars to be observed polarimetrically were selected from the work of Ardeberg & Maurice (1980); we selected representative stars from each one of the stellar groups suggested by those authors in order to have a good coverage in distance moduli. Table 1 lists the selected stars and their memberships. Observations in the *UBVRI* bands were carried out by one of us (E.I.V.) using the VATPOL polarimeter of the Vatican Observatory attached to the 2.15 telescope at the Complejo Astronómico El Leoncito (San Juan, Argentina). Observations were performed on different nights from February through May during the years 1990–1991. Standard stars for null polarization and for the zero point of the polarization position angles are the same as those used by Clocchiatti & Marraco (1988).

Table 2 lists for the observed stars the percentage polarization (P_λ), the position angle of the electric vector (θ_λ) in the equatorial coordinate system, and their respective mean errors for each filter. Also, we indicate in the last column the number of 60 s integrations with each filter. Star numbers are taken from the cited literature.

[1]Based on observations obtained at the Complejo Astronómico El Leoncito, operated under agreement among the Consejo Nacional de Investigaciones Científicas y Técnicas de la República Argentina, Secretaría de Ciencia y Tecnología de la Nación and the National Universities of La Plata, Córdoba and San Juan.
[2]Member of the "Carrera del Investigador Científico" of CONICET, Argentina.

 0004-6256/94/108(5)/1834/9/$0.90

TABLE 1. Membership to the different stellar groups following Ardeberg and Maurice.

Stellar Group	*	$V_0 - M_v \pm \epsilon$
Nearby Group	*12*, 35, 66, *100*	9.22 ± 0.18
7-Star Group	*23*, *30*, *54*, *59*	11.10 ± 0.14
North Group	*43*, 62	12.06 ± 0.29
Group I	29, *31*, 33, 36	12.43 ± 0.18
Group II	46, 51, 67, 77	12.51 ± 0.14
Group III	70, *90*, 92	12.63 ± 0.14
Bright Rim Group	2, 3, 5, 13	12.70 ± 0.28
Group IV	109, 113, 122, 124	12.96 ± 0.14
Aggregate?	104	10.90 ± —

Note to Table 1:

$V_0 - M_v$: taken from Ardeberg & Maurice (1980).

Spectral types and photometry can be found in Ardeberg & Maurice (1980), as well as useful information about individual stars.

3. RESULTS

In the direction to the aggregate, the solar vicinity shows the largest absorption gradient and dispersion that amounts 0.25 mag in $E_{(B-V)}$ over 500 pc; at greater distances, the interstellar absorption is negligible, raising again up to 0.35 from 1 to 1.3 kpc and with a smooth and slow increase farther out. For distances greater than 4 kpc, the interstellar absorption seems pronouncedly patchy.

Following Marraco *et al.* (1993), we intend to remove the effect of the interstellar dust located in front of the aggregate, leaving only the *intra-arm* variations of the interstellar extinction. In order to do so, we have selected among the IC 2944 member stars, a group of nine stars which seems to be the least affected by reddening. These stars, which are hereafter referred to as *frontside* stars, are listed in italics in Tables 1 and 2. They will be used to model the contribution of the foreground excess and polarization, which subsequently will be removed from the remaining member stars to determine the *intra-arm* values of these quantities.

Figure 1 shows the galactic distribution (l,b) of all the stars in the aggregate from the work of Ardeberg & Maurice (1977a, b; 1980). We have used circles for stars with polarimetric measures and triangles for the remaining objects. The stars we have selected as *frontside* are shown as filled circles.

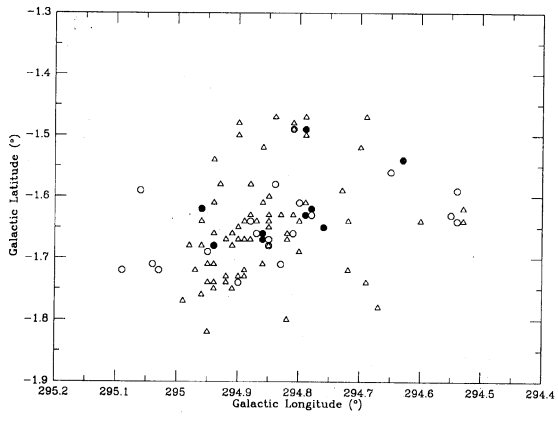

FIG. 1. Galactic distribution of all the stars in the aggregate from the work of Ardeberg & Maurice (1977a, b; 1980). We used circles for stars with polarimetric measures and triangles for the remaining objects. Filled circles indicate our "frontside" stars.

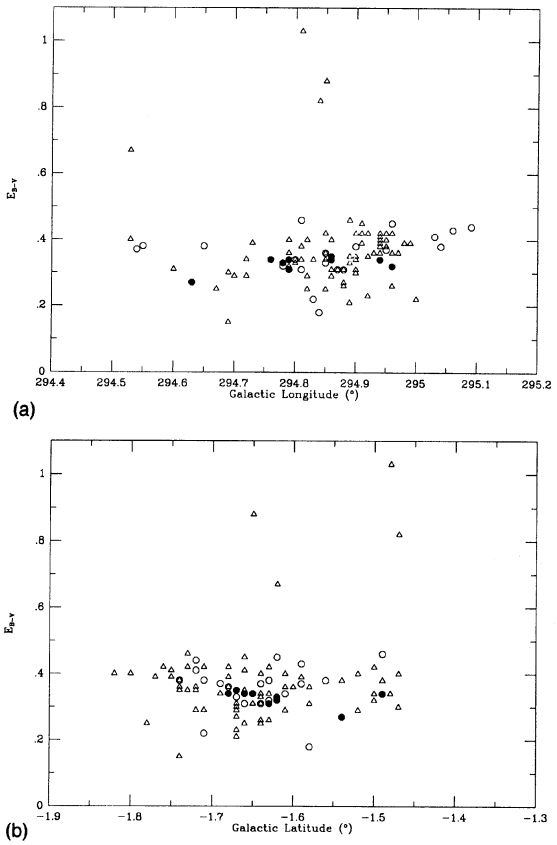

FIG. 2. (a) Color excesses $E_{(B-V)}$ plotted as a function of galactic longitude (l). Excesses are taken from Ardeberg & Maurice (1980). Symbols are the same as in Fig. 1. (b) Color excesses $E_{(B-V)}$ plotted as a function of galactic latitude (b). Excesses and symbols are as in (a).

Figures 2(a) and 2(b) show the color excesses $E_{(B-V)}$ plotted as a function of galactic longitude and latitude, respectively. Excesses are taken from Ardeberg & Maurice (1980) and symbols are the same as in Fig. 1. As can be seen, the excesses show a greater variation in longitude rather than in latitude. It is clear that there are a number of stars that we

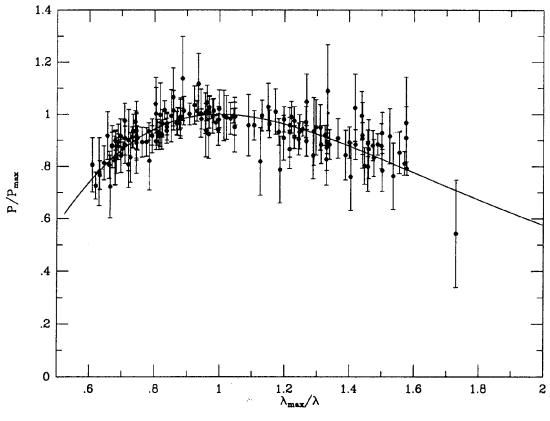

FIG. 3. Normalized wavelength dependence for the observed stars.

TABLE 2. *UBVRI* polarimetric observations.

HD	CPD	LS	⋆	λ	$P_\lambda \pm \epsilon$	$\theta_\lambda \pm \epsilon$	n
	-62°2125		2	0.374	1.65 ± 0.17	92.5± 2.8	1
				0.443	2.02 ± 0.07	90.9± 1.0	1
				0.563	2.08 ± 0.08	91.0± 1.1	1
				0.670	1.89 ± 0.07	92.7± 1.0	1
				0.792	1.85 ± 0.10	90.6± 1.6	1
308692	-62°2130		3	0.374	1.93 ± 0.08	89.4± 1.2	2
				0.443	1.98 ± 0.08	90.1± 1.2	1
				0.563	2.17 ± 0.09	89.9± 1.1	1
				0.670	2.02 ± 0.07	89.0± 1.0	1
				0.792	2.01 ± 0.09	90.3± 1.3	1
			5	0.374	2.20 ± 0.18	91.3± 2.3	1
				0.443	1.65 ± 0.13	89.5± 2.2	1
				0.563	2.29 ± 0.14	88.2± 1.7	1
				0.670	1.79 ± 0.09	86.8± 1.5	1
				0.792	1.57 ± 0.14	97.1± 2.4	1
308688	*-62°2139*		*12*	0.374	1.26 ± 0.08	99.8± 1.9	1
				0.443	1.55 ± 0.06	95.7± 1.1	1
				0.563	1.64 ± 0.07	96.8± 1.2	2
				0.670	1.46 ± 0.05	102.0± 0.9	2
				0.792	1.32 ± 0.08	99.7± 1.7	2
308689	-62°2140		13	0.374	2.33 ± 0.15	106.4± 1.9	1
				0.443	2.35 ± 0.08	109.2± 0.9	1
				0.563	2.38 ± 0.07	108.7± 0.8	1
				0.670	2.24 ± 0.04	107.0± 0.5	1
				0.792	1.78 ± 0.08	106.5± 1.3	1
101084	*-62°2151*	*2417*	*23*	0.374	1.63 ± 0.11	87.4± 1.8	1
				0.443	1.80 ± 0.05	88.4± 0.8	1
				0.563	1.75 ± 0.06	85.0± 0.9	1
				0.670	1.74 ± 0.03	86.3± 0.5	1
				0.792	1.81 ± 0.06	83.4± 1.0	1
	-62°2153	2418	29	0.374	1.45 ± 0.11	90.5± 2.1	1
				0.443	1.74 ± 0.09	89.1± 1.4	1
				0.563	1.78 ± 0.06	92.9± 1.0	1
				0.670	1.54 ± 0.04	92.4± 0.7	1
				0.792	1.58 ± 0.10	93.6± 1.8	1
101131		*2420*	*30*	0.374	1.73 ± 0.08	89.9± 1.3	1
				0.443	1.82 ± 0.02	91.1± 0.8	1
				0.563	1.92 ± 0.02	89.5± 0.3	1
				0.670	1.70 ± 0.02	89.6± 0.4	1
				0.792	1.71 ± 0.03	90.1± 0.5	1
			31	0.374	1.42 ± 0.22	101.1± 4.4	1
				0.443	1.28 ± 0.10	92.9± 2.1	1
				0.563	1.45 ± 0.07	93.5± 1.3	2
				0.670	1.44 ± 0.07	92.0± 1.4	2
				0.792	1.34 ± 0.09	89.0± 1.9	2
308818	-62°2156	2421	33	0.374	1.60 ± 0.12	94.1± 2.1	1
				0.443	1.47 ± 0.09	90.7± 1.8	1
				0.563	1.74 ± 0.10	92.3± 1.6	2
				0.670	1.73 ± 0.10	93.4± 1.6	1
				0.792	1.57 ± 0.14	91.0± 2.5	1
			35	0.374	1.40 ± 0.05	94.3± 1.1	10
				0.443	1.44 ± 0.04	96.3± 0.8	8
				0.563	1.62 ± 0.04	97.0± 0.7	7
				0.670	1.47 ± 0.03	94.4± 0.7	6
				0.792	1.39 ± 0.05	94.5± 1.0	6
308813	-62°2422		36	0.374	1.64 ± 0.08	98.0± 1.3	2
				0.443	1.82 ± 0.06	96.9± 0.9	2
				0.563	1.82 ± 0.04	97.0± 0.6	3
				0.670	1.70 ± 0.04	96.2± 0.7	2
				0.792	1.63 ± 0.07	95.9± 1.1	2
101190	*-62°2163*	*2424*	*43*	0.374	1.76 ± 0.07	90.5± 1.1	2
				0.443	1.99 ± 0.06	89.1± 0.8	2
				0.563	2.15 ± 0.03	92.6± 0.4	2
				0.670	2.09 ± 0.03	91.7± 0.4	2
				0.792	2.10 ± 0.07	90.5± 0.9	2
101191		2425	46	0.374	1.60 ± 0.12	90.9± 2.0	1
				0.443	1.70 ± 0.08	92.8± 1.3	1
				0.563	1.77 ± 0.06	91.7± 0.9	1
				0.670	1.58 ± 0.08	92.8± 1.5	1
				0.792	1.44 ± 0.10	90.8± 1.9	1
	-62°2166		51	0.374	1.52 ± 0.11	90.7± 2.1	1
				0.443	1.58 ± 0.10	91.2± 1.8	1
				0.563	1.76 ± 0.08	93.1± 1.2	1
				0.670	1.72 ± 0.05	91.0± 0.8	1
				0.792	1.67 ± 0.09	89.4± 1.4	1
	-62°2166	*2426*	*54*	0.374	1.63 ± 0.09	89.9± 1.6	2
				0.443	1.70 ± 0.07	87.7± 1.2	2
				0.563	1.85 ± 0.05	88.2± 0.7	2
				0.670	1.70 ± 0.04	90.1± 0.7	2
				0.792	1.47 ± 0.08	86.6± 1.5	2
101205	*-62°2168*	*2427*	*59*	0.374	1.27 ± 0.03	93.2± 0.6	2
				0.443	1.39 ± 0.02	92.8± 0.4	2
				0.563	1.42 ± 0.01	91.7± 0.3	2
				0.670	1.49 ± 0.03	91.5± 0.5	2
				0.792	1.28 ± 0.01	91.7± 0.3	2
101223	-62°2171	2428	62	0.374	1.89 ± 0.05	83.0± 0.7	2
				0.443	2.13 ± 0.10	83.7± 1.3	2
				0.563	2.36 ± 0.05	85.0± 0.6	2
				0.670	2.35 ± 0.08	86.7± 0.9	2
				0.792	2.17 ± 0.10	87.8± 1.3	2
308812			66	0.374	2.12 ± 0.13	91.1± 1.8	2
				0.443	2.05 ± 0.09	92.7± 1.2	2
				0.563	2.23 ± 0.07	92.6± 0.8	2
				0.670	2.20 ± 0.05	91.9± 0.6	2
				0.792	2.07 ± 0.10	91.9± 1.4	2
			67	0.374	1.17 ± 0.09	93.8± 2.3	2
				0.443	1.57 ± 0.12	91.1± 2.2	2
				0.563	1.53 ± 0.07	89.6± 1.4	3
				0.670	1.42 ± 0.04	93.4± 0.9	2
				0.792	1.32 ± 0.08	91.4± 1.6	2
			70	0.374	1.31 ± 0.10	84.6± 2.2	2
				0.443	1.47 ± 0.09	88.7± 1.7	2
				0.563	1.59 ± 0.06	85.4± 1.1	2
				0.670	1.52 ± 0.07	83.0± 1.5	2
				0.792	1.32 ± 0.09	87.2± 1.9	2
			77	0.374	1.29 ± 0.19	99.6± 3.9	2
				0.443	1.61 ± 0.14	91.9± 2.5	1
				0.563	1.67 ± 0.10	97.3± 1.7	2
				0.670	1.72 ± 0.09	99.0± 1.4	3
				0.792	1.41 ± 0.13	93.9± 2.5	2
			90	0.374	1.35 ± 0.12	93.1± 2.5	2
				0.443	1.39 ± 0.11	92.6± 2.2	1
				0.563	1.98 ± 0.04	94.6± 0.6	1
				0.670	1.45 ± 0.07	96.5± 1.4	1
				0.792	1.28 ± 0.11	93.0± 2.3	1
101298	*-62°2186*	2431	92	0.374	1.40 ± 0.07	90.1± 0.6	1
				0.443	1.57 ± 0.07	90.3± 1.3	1
				0.563	1.60 ± 0.07	90.5± 1.1	1
				0.670	1.44 ± 0.05	88.3± 1.0	1
				0.792	1.21 ± 0.07	91.2± 1.6	1
308822	*-62°2193*		*100*	0.374	1.12 ± 0.10	90.9± 2.5	1
				0.443	0.99 ± 0.06	89.7± 1.6	1
				0.563	1.09 ± 0.06	88.5± 1.6	1
				0.670	1.00 ± 0.03	86.9± 1.0	1
				0.792	0.96 ± 0.05	87.2± 1.6	1
308823	-62°2195		104	0.374	1.01 ± 0.10	84.2± 2.7	1
				0.443	0.92 ± 0.08	85.3± 2.4	1
				0.563	1.06 ± 0.07	85.0± 1.9	1
				0.670	1.10 ± 0.04	84.8± 1.1	1
				0.792	1.04 ± 0.09	82.9± 2.4	1
308832	-62°2201		109	0.374	0.52 ± 0.17	102.8± 9.5	1
				0.443	0.82 ± 0.07	97.9± 2.4	1
				0.563	0.98 ± 0.04	94.6± 1.3	2
				0.670	0.88 ± 0.05	96.9± 1.6	1
				0.792	0.95 ± 0.07	92.6± 2.2	1
101413	-62°2205	2438	113	0.374	0.92 ± 0.04	91.6± 1.2	3
				0.443	0.80 ± 0.03	90.0± 1.0	4
				0.563	0.93 ± 0.03	86.6± 0.8	3
				0.670	0.96 ± 0.05	86.8± 1.3	2
				0.792	0.76 ± 0.05	84.3± 1.8	2
308833	-62°2216	2443	122	0.374	1.28 ± 0.14	95.5± 3.1	1
				0.443	1.29 ± 0.09	95.3± 2.1	1
				0.563	1.30 ± 0.11	99.2± 2.3	1
				0.670	1.39 ± 0.10	102.4± 2.0	1
				0.792	1.16 ± 0.11	98.5± 2.7	1
		2444	124	0.374	1.14 ± 0.10	95.9± 2.4	1
				0.443	1.17 ± 0.08	91.3± 1.9	2
				0.563	1.30 ± 0.06	93.0± 1.4	2
				0.670	0.98 ± 0.05	97.5± 1.5	2
				0.792	0.98 ± 0.07	95.4± 2.1	2

Notes to TABLE 2

HD: Henry Draper
CPD: Cape Photographic Durchmusterung.
LS: Luminous Stars (Stephenson & Sanduleak 1977).
⋆: Identification from Ardeberg & Maurice (1977).
λ: Wavelength in μm.
P_λ, θ_λ: Polarization in percent, equatorial position angle in degrees, at λ.

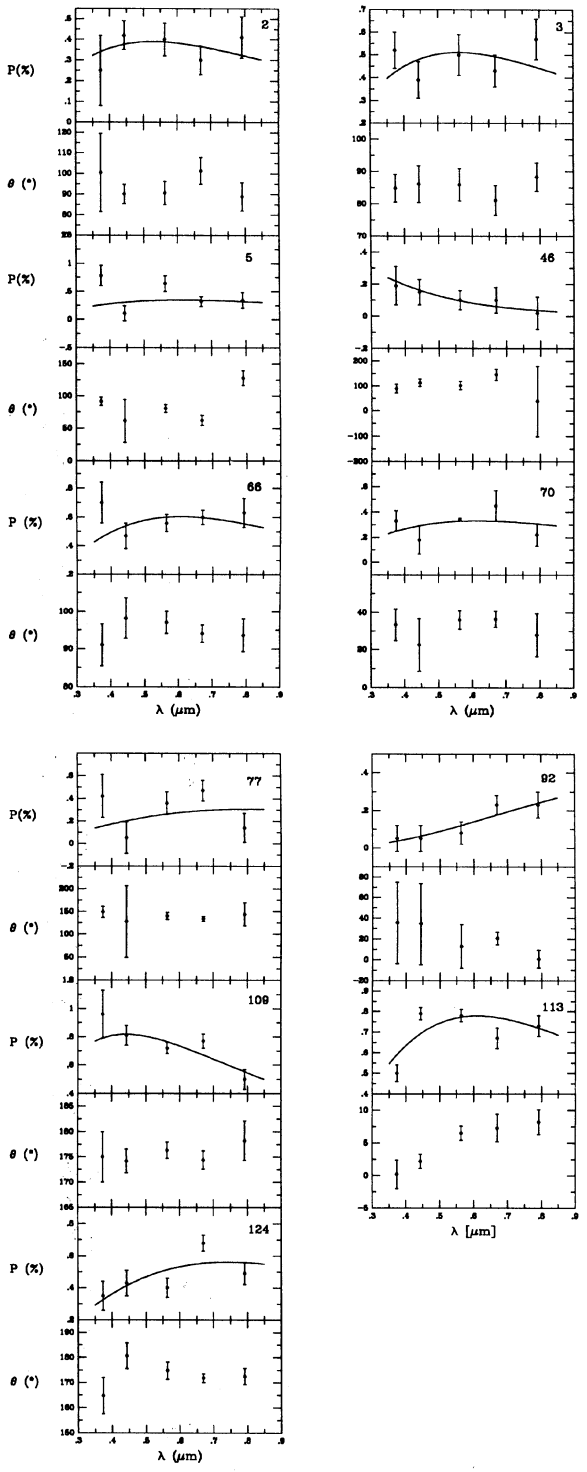

FIG. 4. Polarization and position angle dependence with wavelength for stars with suspected intrinsic polarization.

consider "foreground" to the IC 2944 stellar aggregate. All but two have only measured color excesses; those foreground stars that also have observed polarization are stars No. 35 and 66. Figures 2(a) and 2(b) were used to select the *frontside* stars, following the same criteria as in Marraco

TABLE 3. Observed and intra-arm color excesses and visual polarizations.

HD	CPD	LS	⋆	E_{B-V} O	F	I	Observed $P_v\pm\epsilon$	$\theta_v\pm\epsilon$	Intra-arm $P_v\pm\epsilon$	$\theta_v\pm\epsilon$
	-62°2125		2	.37	.29	.08	2.08 ±.08	91.0±1.1	0.40±.08	90.6± 5.6
308692	-62°2130		3	.38	.29	.09	2.17 ±.09	89.9±1.1	0.50±.09	85.9± 5.0
			5	.37	.29	.08	2.29 ±.14	88.2±1.7	0.64±.14	80.6± 6.1
308689	-62°2140		13	.38	.30	.08	2.38 ±.07	108.7±0.8	1.40±.07	130.6± 1.4
	-62°2153	2418	29	.32	.32	.00	1.78 ±.06	92.9±1.0	0.15±.06	115.1±11.2
308818	-62°2156	2421	33	.31	.33		1.74 ±.10	92.3±1.6	0.09±.10	117.4±31.1
			35	.22	.33		1.62 ±.04	97.0±0.7	0.34±.04	143.9± 3.3
308813	-62°2158	2422	36	.34	.32	.02	1.82 ±.04	97.0±0.6	0.39±.04	128.4± 2.9
101191		2425	46	.36	.34	.02	1.77 ±.06	91.7±0.9	0.10±.06	102.2±16.8
	-62°2166		51	.33	.33	.00	1.76 ±.08	93.1±1.2	0.14±.08	120.7±16.0
101223	-62°2171	2428	62	.46	.32	.14	2.36 ±.05	85.0±0.6	0.75±.06	76.7± 2.2
308812			66	.18	.33		2.23 ±.07	92.6±0.8	0.56±.06	97.1± 3.0
			67	.31	.34		1.53 ±.07	89.6±1.4	0.18±.07	14.6±10.9
			70	.38	.35	.03	1.59 ±.06	85.4±1.1	0.34±.06	36.0± 4.9
			77	.31	.34		1.67 ±.10	97.3±1.7	0.36±.10	139.8± 7.8
101298	-62°2186	2431	92	.34	.35		1.60 ±.07	90.5±1.1	0.08±.06	12.8±21.0
308823	-62°2195		104	.45	.35	.10	1.06 ±.07	85.0±1.9	0.68±.07	10.7± 2.9
308832	-62°2201		109	.41	.36	.05	0.98 ±.04	94.6±1.3	0.72±.04	176.3± 1.6
101413	-62°2205	2438	113	.38	.36	.02	0.93 ±.03	86.6±0.8	0.78±.03	6.5± 1.1
308833	-62°2216	2443	122	.44	.37	.07	1.30 ±.11	99.2±2.3	0.56±.10	161.0± 5.0
		2444	124	.43	.36	.07	1.30 ±.06	93.0±1.4	0.40±.06	174.8± 4.2

Notes to TABLE 3

HD: Henry Draper.
CPD: Cape Photographic Durchmusterung.
LS: Luminous Stars (Stephenson & Sanduleak 1971).
⋆: Identifications from Ardeberg & Maurice (1977a).
E_{B-V}: $B-V$ color excess.
O,F,I: Observed, Foreground (compute from position), Intra-arm.
P_v, θ_v: Polarization in percent, equatorial position angle in degrees, in V.

et al. (1993), that is: they are members of the aggregate according to the different authors, and are the least affected by intracluster reddening.

A least squares fit of the color excesses for the nine *frontside* stars to a plane (l,b) was made in order to model the

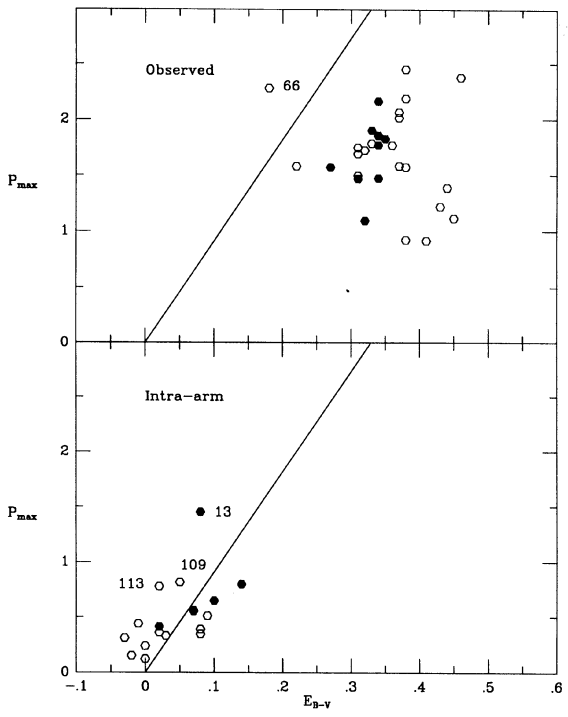

FIG. 5. Polarization efficiency diagram for the observed and *intra-arm* dust. Using R_v=3.1, the line of maximum efficiency is drawn in both diagrams. Filled circles indicate our *frontside* stars in the upper panel, while in the lower one they are used for stars with σ_1<2. Note that star No. 66 is outside the limits of the figure.

TABLE 4. P_{max} and λ_{max} for frontside stars.

HD	CPD	LS	⋆	$P_{max}\pm\epsilon$	$\lambda_{max}\pm\epsilon$
308688	*−62°2139*		*12*	1.569±0.033	0.541±0.020
101084	*−62°2151*	*2417*	*23*	1.856±0.062	0.561±0.037
101131		*2420*	*30*	1.902±0.042	0.539±0.023
			31	1.466±0.035	0.589±0.030
101190	*−62°2163*	*2424*	*43*	2.164±0.029	0.587±0.019
	−62°2166	*2426*	*54*	1.824±0.022	0.524±0.012
101205	*−62°2168*	*2427*	*59*	1.470±0.023	0.555±0.015
			90	1.771±0.147	0.526±0.095
308822	*−62°2193*		*100*	1.092±0.040	0.530±0.032

Notes to TABLE 4

HD: Henry Draper.
CPD: Cape Photographic Durchmusterung.
LS: Luminous Stars (Stephenson & Sanduleak 1978).
⋆: Identification from Ardeberg & Maurice (1977a).
λ_{max}: Wavelength of maximum polarization in μm.

effects of the foreground extinction. The resulting equation is

$$E_{(B-V)}(l,b)=0.12926l-0.06080b-37.8790 \ \text{(mag)} \quad (1)$$

with an rms error of the unit weight of 0.018. As expected, the variation of the excesses with galactic longitude is the most significant part of the model. Table 3 lists observed, modeled and *intra-arm* values of the color excesses for the *non-frontside* stars. It can be noted that our model of the frontside excess led to small or practically negligible values of intra-arm excesses, in accordance with the previous knowledge about dust distribution along the line of sight.

By observing the amount of interstellar polarization in several bandpasses, the wavelength at which maximum polarization P_{max} occurs can be computed. This wavelength λ_{max} is a function of the optical properties and characteristic particle-size distribution of the aligned grains (McMillan 1978; Wilking *et al.* 1980). The maximum polarization (in microns) at which P_{max} (in percentage) occurs has been calculated by fitting the observed interstellar polarization in *UBVRI* bandpasses to the standard Serkowski polarization law (Serkowski 1973):

$$P_\lambda/P_{max}=\exp[-k\ \ln^2(\lambda_{max}/\lambda)], \quad (2)$$

adopting $k=1.15$. Table 4 lists the P_{max} and λ_{max} values for the nine stars selected as *frontside*, whereas the values for the remaining stars can be found in Table 6.

The normalized polarization wavelength dependence of the stars determined from the observations is shown in Fig. 3. The solid curve denotes the Serkowski polarization relation for the general interstellar medium. According to that plot, there exists a good agreement which indicates that the observed polarization is mainly due to the same Davis–Greenstein mechanism that operates in the medium.

The weighted mean of the λ_{max} value for the nine *frontside* stars (star No. 90 was given less weight) is

$$\overline{\lambda_{max}}=0.550\pm0.025\mu. \quad (3)$$

This value is similar to that found by Whittet (1977) for the Carina region: $0.546\pm0.007\mu$. Therefore, it follows that the characteristic particle-size distribution as indicated by the polarization of the stars in the aggregate is essentially the same as that for the diffuse interstellar medium. For the polarization, we get a mean value

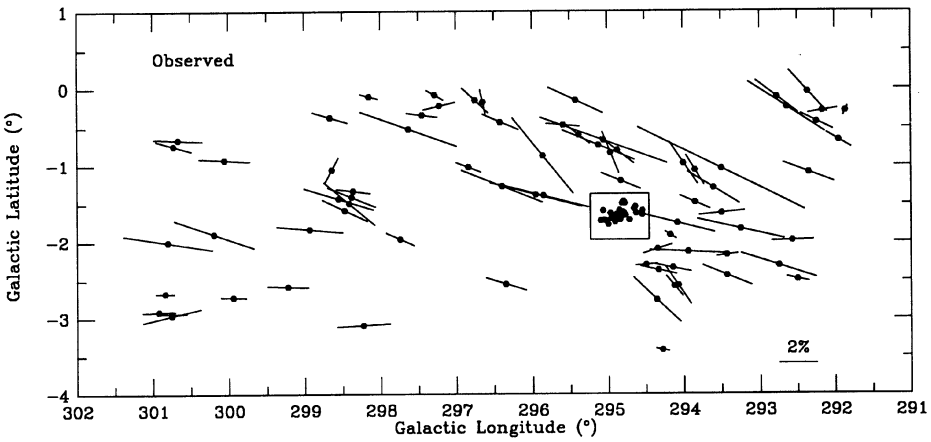

FIG. 6. Polarization vectors and their orientations for stars from the catalogue of Klare & Neckel (1977) in the neighborhood of IC 2944. The length of each vector is proportional to the percentage of polarization. The aggregate itself is located inside the rectangular area.

TABLE 5. *UBVRI* intra-arm polarization.

HD	CPD	LS	⋆	λ	$P_\lambda \pm \epsilon$	$\theta_\lambda \pm \epsilon$	HD	CPD	LS	⋆	λ	$P_\lambda \pm \epsilon$	$\theta_\lambda \pm \epsilon$
	-62°2125		2	0.374	0.25 ±0.17	100.5 ± 19.0	101223	-62°2171	2428	62	0.374	0.66 ±0.05	64.6 ± 2.1
				0.443	0.42 ±0.07	90.1 ± 4.7					0.443	0.72 ±0.10	66.5 ± 3.9
				0.563	0.40 ±0.08	90.6 ± 5.6					0.563	0.75 ±0.06	76.7 ± 2.2
				0.670	0.30 ±0.07	101.3 ± 6.5					0.670	0.80 ±0.08	77.7 ± 2.8
				0.792	0.41 ±0.10	88.8 ± 6.8					0.792	0.76 ±0.10	81.5 ± 3.7
308692	-62°2130		3	0.374	0.52 ±0.08	84.8 ± 4.3	308812			66	0.374	2.12 ±0.14	91.1 ± 5.6
				0.443	0.39 ±0.08	86.1 ± 5.7					0.443	2.05 ±0.09	92.7 ± 5.4
				0.563	0.50 ±0.09	85.9 ± 5.0					0.563	2.23 ±0.07	92.6 ± 3.0
				0.670	0.43 ±0.07	81.1 ± 4.6					0.670	2.20 ±0.05	91.9 ± 2.3
				0.792	0.57 ±0.09	88.3 ± 4.4					0.792	2.07 ±0.10	91.9 ± 4.4
			5	0.374	0.78 ±0.18	91.7 ± 6.5				67	0.374	0.27 ±0.09	169.1 ± 9.3
				0.443	0.11 ±0.13	61.6 ± 33.1					0.443	0.03 ±0.12	181.1 ±112.0
				0.563	0.64 ±0.14	80.6 ± 6.1					0.563	0.18 ±0.07	194.6 ± 10.9
				0.670	0.32 ±0.09	62.2 ± 7.9					0.670	0.22 ±0.04	165.5 ± 5.1
				0.792	0.34 ±0.14	127.9 ± 11.5					0.792	0.12 ±0.08	177.9 ± 18.7
308689	-62°2140		13	0.374	1.32 ±0.15	122.9 ± 3.2				70	0.374	0.33 ±0.10	33.4 ± 8.5
				0.443	1.42 ±0.08	129.9 ± 1.6					0.443	0.18 ±0.09	22.6 ± 14.0
				0.563	1.40 ±0.07	130.6 ± 1.4					0.563	0.34 ±0.06	36.0 ± 4.9
				0.670	1.22 ±0.04	129.1 ± 0.9					0.670	0.45 ±0.07	36.4 ± 4.4
				0.792	0.92 ±0.08	133.3 ± 2.4					0.792	0.22 ±0.09	27.9 ± 11.5
	-62°2153	2418	29	0.374	0.05 ±0.11	71.7 ± 61.6				77	0.374	0.42 ±0.19	149.0 ± 12.7
				0.443	0.19 ±0.09	71.0 ± 13.3					0.443	0.05 ±0.14	127.8 ± 78.4
				0.563	0.15 ±0.06	115.1 ± 11.2					0.563	0.36 ±0.10	139.8 ± 7.8
				0.670	0.10 ±0.04	158.2 ± 11.2					0.670	0.47 ±0.09	133.3 ± 5.4
				0.792	0.19 ±0.10	114.0 ± 14.7					0.792	0.14 ±0.13	143.5 ± 26.0
308818	-62°2156	2421	33	0.374	0.24 ±0.12	113.1 ± 14.0	101298	-62°2186	2431	92	0.374	0.05 ±0.07	35.6 ± 39.2
				0.443	0.12 ±0.09	5.8 ± 21.0					0.443	0.05 ±0.07	34.6 ± 39.2
				0.563	0.09 ±0.10	117.4 ± 31.1					0.563	0.08 ±0.06	12.8 ± 21.0
				0.670	0.19 ±0.10	115.4 ± 14.7					0.670	0.23 ±0.05	20.4 ± 6.1
				0.792	0.13 ±0.14	89.9 ± 30.2					0.792	0.23 ±0.07	0.6 ± 8.5
			35	0.374	0.16 ±0.05	139.9 ± 8.8	308823	-62°2195		104	0.374	1.01 ±0.10	84.2 ± 5.6
				0.443	0.31 ±0.04	153.2 ± 3.6					0.443	0.92 ±0.08	85.3 ± 3.2
				0.563	0.34 ±0.04	143.9 ± 3.3					0.563	1.06 ±0.07	85.0 ± 2.9
				0.670	0.22 ±0.04	156.6 ± 5.1					0.670	1.10 ±0.04	84.8 ± 1.9
				0.792	0.18 ±0.05	147.5 ± 7.8					0.792	1.04 ±0.09	82.9 ± 4.8
			36	0.374	0.43 ±0.08	124.0 ± 5.2	308832	-62°2201		109	0.374	0.52 ±0.17	102.8 ± 5.0
				0.443	0.41 ±0.06	122.4 ± 4.1					0.443	0.82 ±0.07	97.9 ± 2.4
				0.563	0.39 ±0.04	128.4 ± 2.9					0.563	0.98 ±0.04	94.6 ± 1.6
				0.670	0.31 ±0.04	129.5 ± 3.6					0.670	0.88 ±0.05	96.9 ± 1.8
				0.792	0.32 ±0.06	120.2 ± 5.3					0.792	0.95 ±0.07	92.6 ± 3.9
101191		2425	46	0.374	0.19 ±0.12	89.4 ± 17.7	308833	-62°2216	2443	122	0.374	1.28 ±0.14	95.5 ± 15.7
				0.443	0.15 ±0.08	112.8 ± 14.9					0.443	1.29 ±0.09	95.3 ± 6.8
				0.563	0.10 ±0.06	102.2 ± 16.8					0.563	1.30 ±0.11	99.2 ± 5.0
				0.670	0.10 ±0.08	145.3 ± 22.4					0.670	1.39 ±0.10	102.4 ± 4.5
				0.792	0.02 ±0.10	38.9 ±140.0					0.792	1.16 ±0.11	98.5 ± 7.0
	-62°2166		51	0.374	0.11 ±0.12	85.4 ± 30.5			2444	124	0.374	0.35 ±0.09	164.8 ± 7.2
				0.443	0.02 ±0.10	170.3 ±140.0					0.443	0.43 ±0.08	180.6 ± 5.2
				0.563	0.14 ±0.08	120.7 ± 16.0					0.563	0.40 ±0.06	174.8 ± 4.2
				0.670	0.12 ±0.05	89.6 ± 11.7					0.670	0.68 ±0.05	171.8 ± 2.1
				0.792	0.25 ±0.09	79.2 ± 10.1					0.792	0.49 ±0.07	172.5 ± 4.0

Notes to TABLE 5

HD: Henry Draper
CPD: Cape Photographic Durchmusterung.
LS: Luminous Stars (Stephenson & Sanduleak 1977).

⋆: Identification from Ardeberg & Maurice (1977a).
λ: Wavelength in μm.
$P_\lambda, \theta_\lambda$: Polarization in percent, equatorial position angle in degrees, at λ.

$$\overline{P_{max}} = 1.68 \pm 0.031 \quad (4)$$

for the nine selected stars.

Through the use of the Serkowski relation (2), we can calculate a distribution $\overline{P_\lambda}$ for each bandpass that should characterize the *frontside* stars, in the mean. And then, it is possible to calculate mean Stokes parameters $\overline{Q_\lambda}$ and $\overline{U_\lambda}$ for the group. Subtracting this mean value from theindividuals Q_λ and U_λ for the rest of the observed members of IC 2944 and inverting the procedure, we obtain $P_{\text{intra-arm}}(\lambda)$ and $\theta_{\text{intra-arm}}(\lambda)$ values which are listed in Table 5.

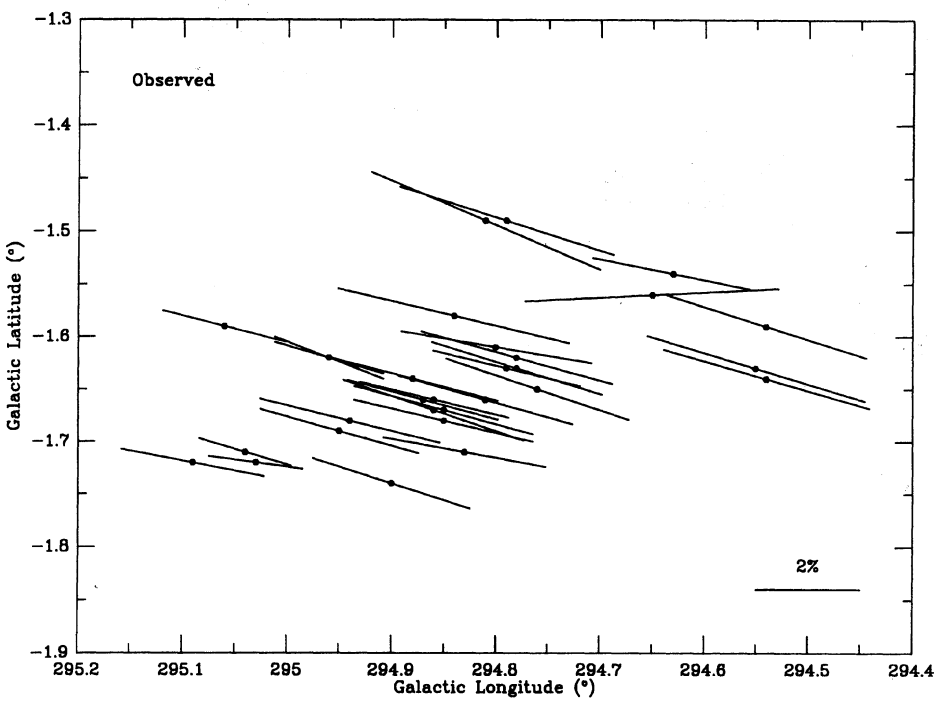

FIG. 7. Rectangular area with observed polarization vectors and their orientations for stars belonging to the IC 2944 aggregate. The length of each vector is proportional to the percentage of polarization.

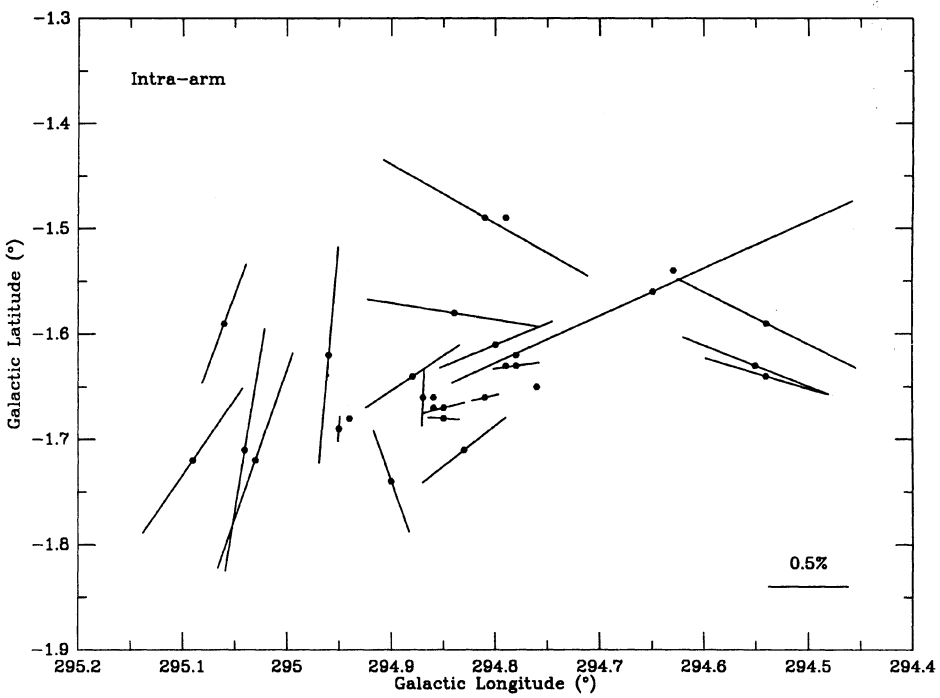

FIG. 8. Intra-arm polarization vectors and their orientations for the IC 2944 stars. The length of each vector is proportional to the percentage of polarization.

TABLE 6. *UBVRI* polarization results.

HD	CPD	LS	⋆	Observed $\lambda_{max}\pm\epsilon$	Observed $P_{max}\pm\epsilon$	Observed σ_1	Intra-arm $\lambda_{max}\pm\epsilon$	Intra-arm $P_{max}\pm\epsilon$	Intra-arm σ_1
	-62°2125		2	.545 ±.021	2.07 ±.04	0.51	.529 ±.099	0.39±.04	2.55
308692	-62°2130		3	.554 ±.022	2.19 ±.04	0.68	.561 ±.094	0.51±.05	2.87
			5	.499 ±.060	2.02 ±.06	1.16	.617 ±.402	0.35±.13	6.31
308689	-62°2140		13	.490 ±.018	2.45 ±.06	0.57	.445 ±.020	1.45±.06	0.70
	-62°2153	2418	29	.519 ±.034	1.72 ±.06	1.03	.614 ±.261	0.12±.02	6.64
308818	-62°2156	2421	33	.570 ±.041	1.75 ±.07	0.86	.482 ±.187	0.15±.04	4.60
			35	.545 ±.019	1.58 ±.03	0.93	.515 ±.119	0.26±.04	6.87
308813		2422	36	.531 ±.017	1.85 ±.03	0.67	.440 ±.038	0.41±.03	1.90
101191		2425	46	.511 ±.010	1.77 ±.02	0.28	.193 ±.070	0.36±.33	5.08
	-62°2166		51	.582 ±.020	1.79 ±.03	0.51	1.334±.822	0.24±.28	8.93
101223	-62°2171		62	.589 ±.004	2.37 ±.01	0.14	.575 ±.023	0.80±.02	0.80
308812			66	.561 ±.026	2.28 ±.05	0.63	.606 ±.095	0.60±.04	2.16
			67	.562 ±.022	1.49 ±.03	0.66	.586 ±.343	0.19±.06	9.90
			70	.552 ±.009	1.57 ±.01	0.24	.615 ±.196	0.33±.06	4.88
			77	.575 ±.027	1.69 ±.04	0.46	.810 ±.692	0.31±.23	8.17
101298	-62°2186	2431	92	.501 ±.010	1.58 ±.02	0.39	1.622±.459	0.44±.31	5.89
308823	-62°2195		104	.589 ±.041	1.11 ±.03	1.10	.509 ±.040	0.65±.03	1.34
308832	-62°2201		109	.665 ±.051	0.92 ±.04	1.49	.443 ±.058	0.82±.08	2.11
101413	-62°2205		113	.538 ±.052	0.92 ±.05	3.11	.610 ±.073	0.78±.06	3.87
308833	-62°2216	2443	122	.539 ±.026	1.39 ±.03	0.59	.787 ±.116	0.55±.08	1.80
		2444	124	.478 ±.036	1.22 ±.07	1.35	.743 ±.145	0.56±.08	3.58

Notes to TABLE 6

HD: Henry Draper.
CPD: Cape Photographic Durchmusterung.
LS: Luminous Stars (Stephenson & Sanduleak 1978).
⋆: Identification as in preceding Tables.
λ_{max}: Wavelength of maximum polarization in μ.
P_{max}: Polarization at λ_{max} in percent.
σ_1: Unit weight error of fit.

Table 6 lists observed and intra-arm P_{max} and λ_{max} values for the non-frontside stars.

To analyze the polarimetric characteristics of the non-frontside objects, we first reject stars with computed intra-arm values of $P_{max}<0.30$, due to their small polarizations in relation to the external errors. For the remaining objects, if the polarization is well represented by the Serkowski relation, σ_1 (the unit weight error of the fit) should not be higher than 2 due to the weighting scheme; a higher value could be indicative of the presence of intrinsic polarization.

11 stars (numbers 2, 3, 5, 46, 66, 70, 77, 92, 109, 113, and 124) in Table 6 have values of the unit weight error above that limit. Figure 4 shows plots of *intra-arm* P and θ vs λ for each one of them, where abnormal Serkowski curves and rather wide variations in the position angle curves can be seen in some of the stars; this suggests a noninterstellar origin of the polarizations. Star No. 36, even when its σ_1 value is less than the critical one, has an extremely low λ_{max} of $0.440\pm0.038\mu$, making it another candidate for a noninterstellar origin of its polarization. In addition, its P vs λ curve resembles that of star No. 109.

There is another indication that the observed polarization for the majority of the observed stars in the aggregate originates in the diffuse interstellar material. Figure 5 shows that the polarization efficiency (ratio of the amount of polarization to the visual extinction) does not exceed the empirical upper limit

$$P_{max}<3A_v\simeq 3R_v E_{(B-V)} \quad (5)$$

derived for the interstellar dust particles (Hiltner 1956), plotted as a solid line. The upper plot corresponds to observed values and excesses taken from cited works, while the lower one reflects the intra-arm situation, with the residual excesses

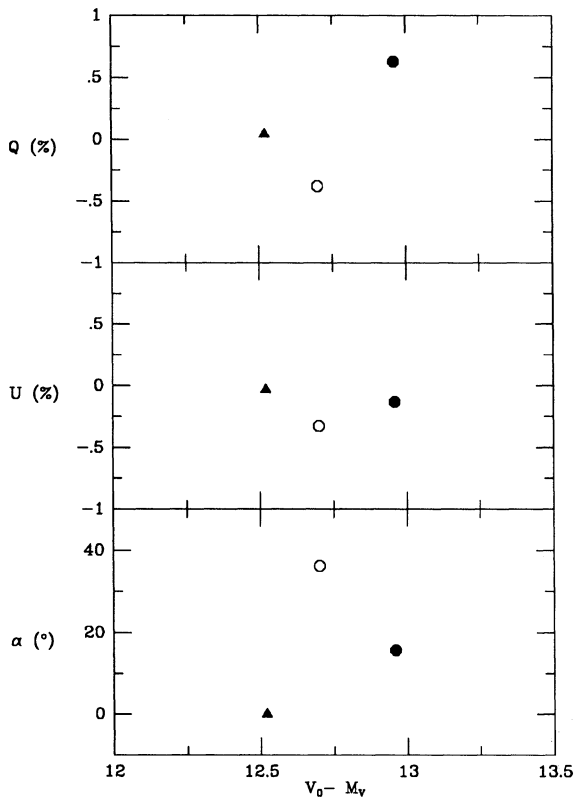

FIG. 9. Parameters of the *intra-arm* polarization plotted as a function of the mean distance moduli for Ardeberg and Maurice's groups. A triangle represents Group I–II–III, while a circle and a filled circle are for the Bright Rim and Group IV, respectively.

coming from Table 3. In the first case, star No. 66 shows a P_{max} value greater than the maximum interstellar limit allowed for its observed color excess. This star was recently mentioned as having a unit weight error in excess of 2. In the other plot, the situation is similar but for stars No. 13, 113 and 109; the last two are mentioned in the paragraph about σ_1. Star No. 13 has passed through all our tests to detect the presence of intrinsic polarization, with only the exception of its position in Fig. 5.

From Fig. 5 it is clear that the *intra-arm* dust produces polarization at a high degree of efficiency. Interpreting the efficiency as proportional to $\cos^2\alpha$, where α is the angle between the plane of the sky and the direction of alignment of the *intra-arm* magnetic field, we can infer that it is mostly contained in the plane of the sky.

When we plot the polarization vectors and their orientations for stars in IC 2944, together with those for stars in its neighborhood (as taken from Klare & Neckel 1977), it is clear that it follows the general trend of the polarization (projected magnetic field) directions in the region (Figs. 6 and 7). The *foreground* polarization has an average direction of 91°.2 in equatorial coordinates. Figure 9 shows the run of the parameters of the *intra-arm* polarization with mean distance moduli for the groups defined by Ardeberg & Maurice (1980). As found by Perry & Landolt (1986), only Group IV

and the Bright Rim Group are significantly different. Group IV is particularly notable in Fig. 8 where all its members have position angles close to 0° in galactic coordinates (stars with $l>294.94°$).

4. CONCLUSIONS

The foreground polarization in the direction to IC 2944 is normal and has a λ_{max} value of $0.550\pm0.025\mu$. Its average direction in equatorial coordinates is 91°.2. About half of the stars not considered to be *frontside* have some indication of intrinsic polarization. Interpreting the polarization of the rest as *intra-arm* polarization, we find that Ardeberg & Maurice's Groups I, II, and III cannot be separated in terms of polarization data and that the Bright Rim Group and Group IV are significantly different.

Finally, stars in Groups I, II, III, and IV show that the *intra-arm* (beyond 1.4 kpc) magnetic field is essentially contained in the plane of the sky.

One of us (E.I.V.) wants to acknowledge the technical support at CASLEO during the observing runs, in particular to night assistant Mr. Antonio De Francescchi, and to Ms. Graciela Salas for her clerical support. Special thanks go to Mrs. S. D. Abal de Rocha and to Mr. Ruben E. Martínez for technical assistance. Also, we gratefully acknowledge the support of the Consejo Nacional de Investigaciones Científicas y Técnicas de la República Argentina.

REFERENCES

Ardeberg, A., & Maurice, E. 1977a, A&A, 54, 233
Ardeberg, A., & Maurice, E. 1977b, A&AS, 28, 153
Ardeberg, A., & Maurice, E. 1980, A&AS, 39, 325
Clocciatti, A., & Marraco, H. G. 1988, A&A, 197, L1
Hiltner W. A. 1956, ApJS, 2, 389
Klare, G., & Neckel, Th. 1977, A&AS, 27, 215
Marraco, H. G., Vega, E. I., & Vrba, F. J. 1993, AJ, 105, 258
McMillan, R. S. 1978, ApJ, 225, 880
Perry, C. L., & Landolt, A. U. 1986, AJ, 92, 844
Serkowski, K. 1973, in Interstellar Dust and Related Topics, Proc. IAU Symposium No. 52 edited by J. M. Greenberg and H. C. van der Hulst (Reidel, Dordrecht), p. 145
Stephenson A., & Sanduleak, N. 1972, Warner and Swasey Obs. I, No. 1
Walborn, N. 1987, AJ, 93, 868
Whittet, D. C. B. 1977, MNRAS, 180, 29
Wilking, B. A., Lebofsky, M. J., Martin, P. G., Rieke, G. H., & Kemp, J. C. 1980, ApJ, 235, 905